COBEM 2023 27TH INTERNATIONAL CONGRESS OF MECHANICAL ENGENEERING

ABCM Brazilian Society of Mechanical Sciences and Engineering
27th ABCM International Congress of Mechanical Engineering
December 04-08, 2023, Florianópolis-SC, Brazil

COB-2023-1234
TOTAL EQUIVALENT WARMING IMPACT OF ALTERNATIVE REFRIGERANTS FOR REPLACEMENT OF R-22

Leonardo Victor Silva Martins
Luiz Machado
Post-Graduate Program in Mechanical Engineering, Federal University of Minas Gerais (UFMG)
Av. Pres. Antônio Carlos, 6627 - Pampulha, Belo Horizonte - MG, 31270-901, Brazil.
leo.vsm@hotmail.com, luizm@ufmg.br

Tiago de Freitas Paulino
Federal Center of Technological Education of Minas Gerais (CEFET-MG), Graduate Program in Mechanical Engineering
Av. Amazonas, 5253 - Nova Suiça, Belo Horizonte - MG, 30421-169, Brazil
tfpaulinoeng@gmail.com

Juan Jose Garcia Pabon
Federal University of Itajuba (UNIFEI), Graduate Program in Mechanical Engineering
Av. BPS, 1303, Bairro Pinheirinho, Itajubá – MG
jjgp@unifei.edu.br

Willian Moreira Duarte
Post-Graduate Program in Mechanical Engineering, Federal University of Minas Gerais (UFMG)
Av. Pres. Antônio Carlos, 6627 - Pampulha, Belo Horizonte - MG, 31270-901, Brazil.
willianmoreira@ufmg.br

Abstract. *The Montreal Protocol and its amendments have been increasingly restricting the use of refrigerant fluids, considering the significant environmental impact they can cause. However, a large portion of refrigeration and air conditioning units in developing countries like Brazil still operate with R-22, and discarding these equipments solely due to the refrigerant would result in not only economic but also environmental damages. In order to reuse these equipments, it is interesting to evaluate alternative refrigerants that, with minor modifications to the system, enable their reuse. Therefore, this study compared the coefficient of performance (COP) of R-22 and some of its alternatives as well as the Total Equivalent Warming Impact. The refrigerants considered were R-407C, R-444B, and R-454C. For this purpose, a lumped model was used for the heat exchangers and the model described in the Canadian standard AHRI 540 was used to the compressor. The average difference of COP was -9.24%, -5.02%, and -13.91% for R-407C, R-444B, and R-454C fluids, respectively. Total Equivalent Warming Impact found was 12.32, 12.37, 9.84 and 10.12 for the refrigerants R-22, R-407C, R-444B, and R-454C, respectively. In conclusion, considering the conditions and data of the study, the best refrigerant for retrofit of R-22 is the R-444B.*

Keywords: *R-22, Mathematical model, HVAC*

1. INTRODUCTION

The Montreal Protocol is an international treaty adopted in 1987 with the aim of regulating the production and use of chemical substances that contribute to the depletion of the ozone layer. This agreement establishes a schedule for the reduction and phasing out of these chemicals, initially signed by 46 countries and currently having approximately 200 signatures (Encyclopaedia Britannica, 2022; EPA, 2021; EPE, 2022).

Since its inception, several amendments have been made to expand its scope and anticipate steps, recognizing the benefits of the protocol for the Earth's climate. In 2007, the members decided to accelerate the phase-out schedule for Hydrochlorofluorocarbons (HCFCs), substances that not only deplete the ozone layer but are also potent greenhouse gases: the most common HCFCs, such as R-22, are approximately 2000 times more potent than carbon dioxide in terms of Global Warming Potential (GWP). Developed countries would reduce the consumption of these substances until complete phase-out by 2020, while developing countries would initiate the same process and complete it by 2030 (UNEP, 2018).

The global phase-out schedule for these refrigerants stimulates the development of new equipment and technologies optimized for this new context. However, a significant portion of refrigeration and air conditioning units in developing countries, such as Brazil, operate with these refrigerants (especially R-22), and discarding such equipment solely because

of the refrigerant would result in significant losses not only for the owners but also for the environment.

In order to reuse these units, it is important to search for alternative refrigerants that can replace the current ones with minimal modifications to the system without significantly compromising the performance of these units.

Therefore, this study aims to compare R-22 with alternative refrigerants (R-407C, R-444B, and R-454C) using a mathematical model to find a substitute refrigerant for both. This would allow for a direct transition, avoiding intermediate steps and, consequently, reducing costs. Parameters such as condenser pressure, refrigerant charge, cooling capacity, COP, and Total Equivalent Warming Impact (TEWI) will be taken into account.

2. METHODOLOGY

For this study, a split-type air conditioning system will be adopted, which consists of two units: the evaporator unit, located inside the Thermal zone and composed of the evaporator and its respective fan; and the condenser unit, located outside and primarily composed of the condenser and its respective fan, compressor, and capillary tube. The connection between these two units is achieved through pipes. Figure 1 illustrates this concept, with (A) providing a perspective drawing and (B) a schematic drawing. In order to evaluate the fluids in this model, there were considered a combination of internal (18ºC, 21ºC, and 24ºc) and external (25ºC to 40ºC) temperatures.

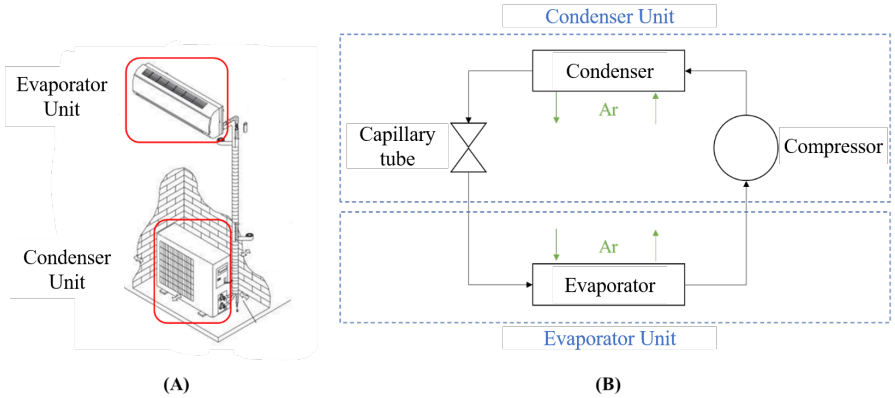

Figure 1. Split-type air conditioning unit: (A) perspective drawing; (B) schematic drawing.

2.1 Alternative refrigerant fluids

As mentioned, the alternative refrigerants considered in this study are R-407C, R-444B, and R-454C. The first one was chosen because it is commonly used as a substitute for R-22 and serves as a reference for comparison. The other two were selected based on existing studies evaluating alternatives to R-22. All of them have no ODP (Ozone Depleting Potential). Table 1 presents some characteristics of these refrigerants (Abdelaziz *et al.*, 2015; Lemmon *et al.*, 2018; Sethi *et al.*, 2015; Kim and Kim, 2021). The proposed fluids can not be used with the same oil as R22 therefore it necessary to change the lubricant in the system. It highlights values for GWP, densities, specific and latent heats, and viscosity, parameters that will be used for result analysis. Although R-410A equipment have been used to replace R-22 equipment, R-410A can not be used to retrofit the R-22 due difference of compressor displacement as shown in the data published by Chen (2008).

2.2 Air conditioner mathematical model

A quasi-steady-state model (steady-state model that incorporates thermal inertia) was developed using a open-code source (Python), based on the model used by Duarte *et al.* (2023) and considering a real system located in the GREA's laboratory of the Federal University of Minas Gerais (UFMG). In this model, pressure losses in the tubes between components were considered negligible, the evaporator and condenser were assumed to be isobaric, and a compact model was adopted. In the next topics, the equations used to describe each component will be presented.

2.2.1 Compressor model

As mentioned by de Paula *et al.* (2021) and Duarte *et al.* (2023), there are various ways to model a compressor, ranging from simpler to more detailed approaches, in the literature. However, the more sophisticated models (Fonseca *et al.*, 2022; Duarte *et al.*, 2019; Yang *et al.*, 2013) require multiple parameters and geometric details that are not typically provided by manufacturers of hermetic compressors. Furthermore, the compressor model adopted for a complete refrigeration system is usually a simplified version, as employed in studies by de Paula *et al.* (2020), Minetto (2011) and Rabelo *et al.* (2019).

Table 1. Properties of R-22, R-407C, R-444B, and R-454C.

Property	**R-22**	**R-407C**	**R-444B**	**R-454C**
Composition	$CHCLF_2$	R-32/R-125/R-134a	R-32/152a/1234ze(E)	R-32/1234yf
Composition (\% by mass)	Pure	20 |40 | 40	41.5 |10 | 48.5	21.5 | 78.5
GWP	1760	1624	295	148
ODP	0.040	0	0	0
Safety group	A1	2	A2L	A2L
Compressor lubricant	Mineral oil	POE oil	POE oil	POE oil
Critical pressure (MPa)	4.99	4.64	5.38	4.32
Critical temperature (ºC)	96.13	86.14	95.62	85.67
Evaporation temperature^a (ºC)	-40.82	-43.90	-45.59	-45.84
Liquid density^a (kg/m^2)	1410	1381	1264	1277
Vapor Density^a (kg/m^2)	4.69	4.57	3.83	4.85
Latent Heat of Vaporization^a (kJ/kg)	234.1	249.3	292.2	227.5
Vapor Viscosity^a ($\mu Pa.s$)	10.13	9.75	9.44	9.00
S. Heat of Vapor Const. Pres. (kJ/kgK)	0.605	0.785	0.842	0.810
S. Heat of Liquid Const. Pres. (kJ/kgK)	1.089	1.312	1.411	1.271

Therefore, the equations provided by the compressor manufacturer for mass flow rate and electrical power in terms of evaporating (T_e) and condensing (T_c) temperatures were used, as defined by the Canadian standard AHRI 540 (AHRI, 2020). The standard equations are indicated in Eqs. (1) and (2), where $\dot{m}_m$ represents the mass flow rate (kg/s) and $\dot{W}_t$ represents the electrical power input (W). The coefficients, denoted by the letter B, are presented in Tab. 2 and correspond to the HGA5512EX model (Tecumseh , 2023).

$$\dot{m}_m = B_A + B_B T_e + B_D T_e^2 + B_G T_e^3 + \left(B_C + B_E T_e + B_H T_e^2\right) T_c + \left(B_F + B_I T_e\right) T_c^2 + B_J T_c^3 \tag{1}$$

$$\dot{W}_m = B_A + B_B T_e + B_D T_e^2 + B_G T_e^3 + \left(B_C + B_E T_e + B_H T_e^2\right) T_c + \left(B_F + B_I T_e\right) T_c^2 + B_J T_c^3 \tag{2}$$

Table 2. Parameters for Eqs. (1) and (2), adapted from (Tecumseh , 2023)

	B_A	B_B	B_C	B_D	B_E
$\dot{m}_m$	1.925049E+02	-9.377586E-01	-1.131359E+00	-8.143320E-02	2.509357E-01
W_m	1.619702E+02	-1.062771E+01	2.574098E+01	-1.496457E+00	4.544785E-01
	B_F	B_G	B_H	B_I	B_J
$\dot{m}_m$	-1.513539E-02	6.137548E-04	5.061497E-03	-3.103936E-03	2.225813E-04
W_m	-3.580018E-01	5.037625E-02	5.019033E-03	-1.063087E-03	3.263633E-03

To determine these equations, the manufacturer conducts tests with the compressor inlet temperature held constant at 35°C. However, this condition is not achieved for lower evaporating temperatures. Therefore, Dabiri and Rice (1981) recommends using Eqs. (3) and (4) to obtain the correct values of mass flow rate and electrical power input.

$$\dot{m}_r = \left(\frac{\rho_r}{\rho_t}\right) \dot{m}_m \tag{3}$$

$$\dot{W}_{cp} = \frac{\dot{m}_r}{\dot{m}_m} \dot{W}_m \tag{4}$$

In these equations, $\dot{m}r$ represents the actual mass flow rate, ρr represents the density (kg/m³) at the compressor inlet (actual value), ρ_t represents the density for the manufacturer's test temperature, and $\dot{W}_{cp}$ represents the actual electrical power input.

2.2.2 Expansion valve model

The expansion device used in this project was the thermostatic expansion valve, and the expansion process was considered as isenthalpic. A superheating value of 7 Kelvin was adopted, which is commonly used in the literature, as in de Paula *et al.* (2020).

2.2.3 Heat exchangers models

Considering the application of heat exchangers in a split-type air conditioning unit, where not all temperatures of the involved fluids are known, the use of the effectiveness-NTU method is recommended (Incropera *et al.*, 2007). Although there are several studies that adopt distributed heat exchanger models (Diniz *et al.*, 2021; Garcia *et al.*, 2018; Paulino *et al.*, 2019), these models require significant computational effort when compared to compact models. Additionally, some studies have shown that compact models can be used to evaluate their performance more quickly (de Paula *et al.*, 2020; Li *et al.*, 2017; Nunes *et al.*, 2015). The energy balance for the refrigerant and air in the heat exchangers (condenser and evaporator) is presented in Eq. (5) (Incropera *et al.*, 2007)

$$\dot{Q} = \dot{m}_r(i_o - i_i) = \dot{m}_a C_{pa}(T_i - T_o) \tag{5}$$

Where $\dot{Q}$ represents the heat transfer rate (W), i is the specific enthalpy of the refrigerant (kJ/kg), ma is the air mass flow rate (kg/s), Cpa is the specific heat capacity of air at constant pressure (W/K), and T is the air temperature (K). The subscripts i and o represent the inlet and outlet of the heat exchanger, respectively.

The first step in this procedure is to determine the maximum possible heat transfer rate, $\dot{Q}_{max}$:

$$\dot{Q}_{max} = \dot{C}_{min}(T_{q,in} - T_{f,in}) \tag{6}$$

where $\dot{C}min$ represents the smaller heat capacity rate (of either the air or the refrigerant), Tq, in is the inlet temperature of the hot fluid, and Tf, in is the inlet temperature of the cold fluid. To calculate the heat capacity rate, the specific heat capacity, cp, and the mass flow rate, $\dot{m}$, are used as indicated in Eq. (7)(Duarte, 2018).

$$\dot{C} = c_p \dot{m} \tag{7}$$

The effectiveness, ε, is defined as the ratio between the actual heat transfer rate in a heat exchanger and the maximum possible heat transfer rate, as indicated in the Eq.(8) (Incropera *et al.*, 2007).

$$\varepsilon = \frac{\dot{Q}}{\dot{Q}_{max}} \tag{8}$$

For the split-type air conditioner (cross-flow heat exchanger without fluid mixing), the effectiveness can also be calculated using the Eq. (9) (ASHRAE, 1997).

$$\varepsilon = 1 - \exp\left[\left(\frac{\dot{C}_{max}}{\dot{C}_{min}}\right)\text{NTU}^{0.22}\left\{\exp\left[-\left(\frac{\dot{C}_{min}}{\dot{C}_{max}}\right)\text{NTU}^{0.78}\right] - 1\right\}\right] \tag{9}$$

The number of transfer units (NTU), indicated in Eq. (9), is a dimensionless parameter defined as stated in Eq. (10) (Incropera *et al.*, 2007).

$$\text{NTU} = \frac{UA}{\dot{C}_{min}} \tag{10}$$

In this equation, A represents the heat exchanger area (m²) and U represents the overall heat transfer coefficient ($Wm^{-2}K^{-1}$) which Duarte *et al.* (2023) suggests calculating using Eq. (11).

$$UA = \left(\frac{1}{\bar{h}_a A_a} + \frac{1}{\bar{h}_r A_r}\right)^{-1} \tag{11}$$

The average heat transfer coefficient of the refrigerant, $\bar{h}r$, is calculated by numerically integrating with respect to specific enthalpy, as performed by Zhang *et al.* (2014). For the condenser, the correlation proposed by Gnielinski (1976) is used when the specific enthalpy, i, is greater than or equal to the vapor enthalpy (iv) or less than or equal to the liquid enthalpy (il), representing single-phase flow. When i is between il and i_v, representing two-phase flow, the correlation proposed by Shah (2022a) is used. For the evaporator, the correlation by Gnielinski (1976) is used for single-phase flow, and the correlation proposed by Shah (2022b) is used for two-phase flow. To implement the correlation by Gnielinski (1976), Neils and Klein (2009) suggests using the correlation proposed by Zigrang and Sylverster (1982) for the Darcy friction factor (f). The average heat transfer coefficient of the air, h_a, is calculated using the correlation by Grimson (1937) for the evaporator, Eq. (12), as recommended by Incropera *et al.* (2007). For the condenser, the correlation by Churchill and Bernstein (1977), Eq. (13), was used, taking into account the geometry of the condenser.

$$\bar{h}_a = B_0 Re_{max}^m Pr^{1/3}(k/D) \tag{12}$$

Table 3. Main parameters for the simulation.

Parameter	Value	Parameter	Value
Evaporator heat exchange area	3.99 m²	Condenser heat exchange area	7.71 m²
Evaporator front area	0.12 m²	Condenser front area	0.18 m²
Evaporator tube lenght	14.4 m	Condenser tube lenth	19.2 m
Evaporator fan power	20 W	Condenser fan power	30 W
Evaporator fan volumetric flow	550 m³/h	Codenser fan volumetric flow	1360 m³/h
Evaporator nominal diameter	5/16 "	Condenser nominal diameter	5/16 "
Compressor diameter	0.120 m	Compressor height	0.203 m
Compressor ratio	35 %	Moisture removal	1 kg/h
Lenght between the units	7,0 m	Copper roughness	1.5E-6 m
Diameter high pressure	1/4 "	Diameter low pressure	3/8 "
Gravity acceleration	9.78 m/s²	Atmospheric pressure	101 kPa
R-22 Charge	0.670 kg	R-407C Charge	0.591 kg
R-444B Charge	0.402 kg	R-454C Charge	0.439 kg

$$\bar{h}_a = 0.3 + \frac{0.62 Re^{0.5} Pr^{1/3}}{\left[1 + (0.4/Pr)^{2/3}\right]^{0.25}} \left[1 + \left(\frac{Re}{282000}\right)^{5/8}\right]^{0.8} \tag{13}$$

where k represents thermal conductivity, D represents the outer diameter of the tube, and Pr represents the Prandtl number. The coefficients B_0 and m vary depending on the tube arrangement (inline/alternate) and the transverse and longitudinal pitches. Considering the geometry of the heat exchangers considered in this study, Re_{max} is calculated using Equation (14) (Incropera *et al.*, 2007).

$$Re_{max} = \frac{2\rho V D}{\mu} \tag{14}$$

where V is the air velocity at the evaporator inlet and μ is the viscosity. Finally, the energy balance to account for the condensation of water present in the air is performed using Eq. (15), as proposed by Duarte *et al.* (2023). In this equation, m_{ce} represents the mass flow rate of condensate in the evaporator. Regarding the heat exchangers information, it is available in Table 3.

$$\dot{Q}_e = \dot{m}_a C_{pa}(T_o - T_i) + \dot{m}_{ce}(i_V - i_L) \tag{15}$$

2.2.4 Refrigerant charge

The refrigerant charge in each component was calculated, and the total charge was considered as the sum of these values. For the pipes, Eq. (16) for the single-phase regime and Eq. (17) for the two-phase regime were used, as suggested by Duarte *et al.* (2023).

$$m = \int \rho d\forall \tag{16}$$

$$m = \int \left[\alpha\rho_v + (1-\alpha)\rho_l\right] d\forall \tag{17}$$

In these equations, the subscripts l and v refer to liquid and vapor, respectively. The void fraction, α, is calculated using the correlation proposed by Hughmark (1965). Eqs. (16) and (17) were numerically integrated, considering constant specific enthalpy for each stage, as done by Duarte *et al.* (2019) and Zhang *et al.* (2014). To assess the refrigerant charge in the pipes, a distance of 7m was considered between the indoor and outdoor units, and 0.3m between components of the outdoor unit.

In these equations, the subscripts l and v refer to liquid and vapor, respectively. The void fraction, α, is calculated using the correlation proposed by Hughmark (1965). Eqs. (16) and (17) were numerically integrated, considering constant specific enthalpy for each stage, as done by Duarte *et al.* (2019) and Zhang *et al.* (2014). For the capillary tube, the same procedure was adopted, with the exception of using the average density between the inlet and outlet.

To calculate the mass inside the compressor, the approach used by Humia *et al.* (2022); **?** was employed, which consists of calculating the free internal volume of the compressor and multiplying it by the density at the suction. To determine this volume, the total volume is calculated based on the dimensions provided by the manufacturer, and a factor is adopted to represent the free space, i.e., the space not occupied by the electromechanical assembly. Finally, to calculate the mass in the condenser and evaporator, the approach proposed by Otaki (1971) was used.

2.3 Performance indicators

The coefficient of performance, or COP, represents the ratio between the cooling capacity and the supplied power. (Bell, 2012) suggests calculating this parameter according to Eq. (18).

$$COP = \frac{\dot{Q}_e - \dot{W}_e}{\dot{W}_{cp} + \dot{W}_e + \dot{W}_c} \tag{18}$$

In this equation, $\dot{Q}_e$ represents the energy absorbed by the evaporator, $\dot{W}e$ is the power consumed by the evaporator fan, $\dot{W}cp$ is the power consumed by the compressor, and $\dot{W}c$ is the power consumed by the condenser fan. Furthermore, to assess the environmental impact of the refrigeration system, the Total Equivalent Warming Impact (TEWI, in kilograms of $CO2$) was used, as indicated by (de Paula *et al.*, 2020; Humia *et al.*, 2021). This parameter considers direct and indirect emissions, as indicated in Eqs. (19), (20), and (21).

$$TEWI_{Total} = TEWI_{Direct} + TEWI_{Indirect} \tag{19}$$

$$TEWI_{Direct} = GWP \cdot m \cdot L_{rate} \cdot L_{time} + GWP \cdot m \cdot (1 - \alpha_{rec}) \tag{20}$$

$$TEWI_{Indireto} = E_{annual} \cdot \beta \cdot L_{time} \tag{21}$$

In them, m represents the refrigerant charge (as indicated in Table 3); L_{rate}, the annual refrigerant emission rate (leakages) (12.5% of total mass, considering a regular operation, catastrophic losses, and maintenance services (AIRAH, 2012)); L_{time}, the system's lifetime (15 years, considering economic life (Makhnatch and Khodabandeh, 2014)); α_{rec}, the annual recovery rate (70%, considering refrigerant charge less than 100kg (AIRAH, 2012)); E_{annual}, the system's annual electricity consumption (kWh/Year); and β, the CO_2 emission factor in electricity production (0.082 $kgCO_2/kWh$, considering the Brazilian reference value (Rees, 2016)). Regarding electricity consumption, it was calculated by summing the energy consumed during each time fraction that the system operated throughout the entire evaluation period (one year - 2022).

3. RESULTS

When comparing the results obtained for the considered fluids, it is evident that the Coefficient of Performance (COP) varies significantly depending on the internal (evaporator inlet) and external (condenser inlet) temperatures, as indicated in Fig.2. However, each fluid exhibits a specific behavior, making it challenging to identify common patterns among them. In order to facilitate the comparison, the average COP values of the alternative fluids were considered in relation to R-22. By doing so, it was possible to identify an average difference of -9.24%, -5.02%, and -13.91% for R-407C, R-444B, and R-454C fluids, respectively.

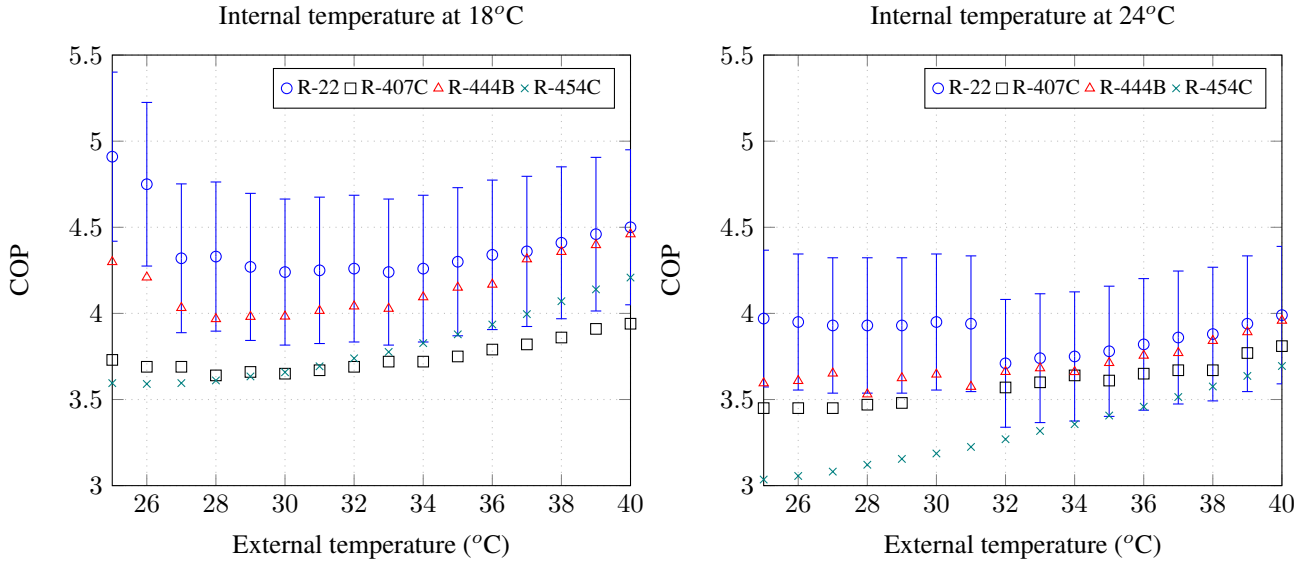

Figure 2. COP for an internal temperature of 18 and 24ºC.

Regarding the cooling capacity, there is a similar behavior among the fluids (Fig.3, with values close to the limit of ±10% compared to the values of R-22 under the same conditions). Thus, the difference between the average values, when compared to R-22, is -2.75%, -5.64%, and -10.26% for R-407C, R-444B, and R-454C fluids, respectively.

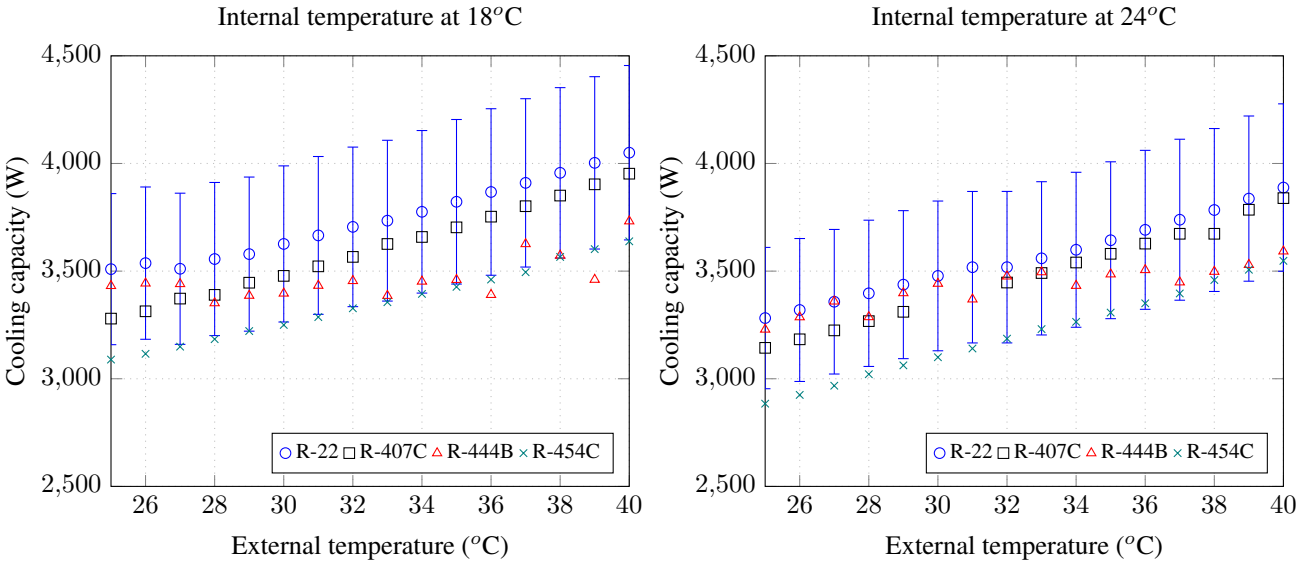

Figure 3. Cooling capacity for an internal temperature of 18 and 24ºC.

Moving on to the Total Equivalent Warming Impact (TEWI) comparison among the four fluids (Fig. 4), a division into two groups can be observed: R-22 and R-407C with virtually identical total TEWI (approximately 12.m ton of CO_2 equivalent), and R-444B and R-454C with a reduction of 20.1% and 17.8%, respectively. It is worth noting that the direct TEWI of these two fluids corresponds to 10% and 5.5% of the R-22 value, respectively, due to their significantly lower Global Warming Potential (GWP) and an average 35% lower refrigerant charge compared to the reference fluid.

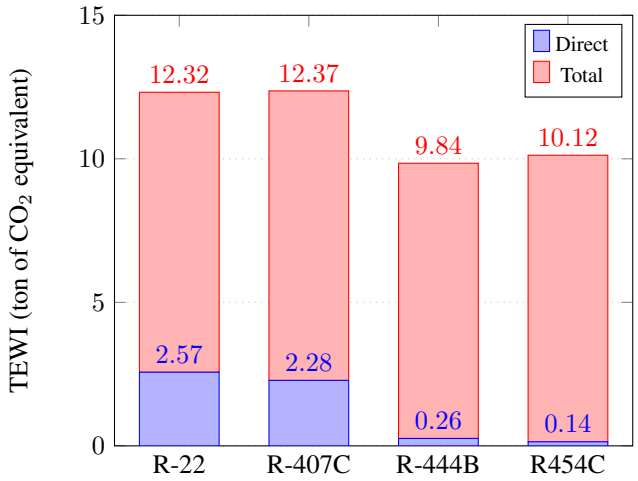

Figure 4. Total TEWI for the four fluids (considering 15 years of lifetime.

4. CONCLUSIONS

In this study, a comparative analysis of COP, Cooling Capacity, and TEWI was conducted for three alternative refrigerant fluids to R-22: R-407C, R-444B, and R-454C. These fluids were evaluated across a combination of two internal temperatures (18°C and 24°C) and sixteen external temperatures (25°C to 40°C). By examining the obtained average values, it was possible to validate that R-444B and R-454C, with their low Global Warming Potential (GWP), exhibited significant potential for replacing R-22.

Finally, it is important to highlight the overall result of R-444B, which among the three alternatives studied for R-22, exhibits the smallest average COP difference (5.02%), an acceptable difference in cooling capacity (-5.64%), and the highest reduction in total TEWI (20.1%). These findings indicate that R-444B is an excellent fluid for further comparative analysis in different scenarios.

5. ACKNOWLEDGEMENTS

This work was supported by Foundation for Research Support of the State of Minas Gerais (FAPEMIG), Brazil and National Council for Scientific and Technological Development (CNPq), Brazil. This study was financed in part by the Coordenação de Aperfeiçoamento de Pessoal de Nível Superior - Brasil (CAPES) - Finance Code 001.

6. REFERENCES

Abdelaziz, O., Shrestha, S., Munk, J., Linkous, R., Goetzler, W., Guernsey, M. and Kassuga, T., 2015. "Alternative refrigerant evaluation for high-ambient-temperature environments: R-22 and r-410a alternatives for mini-split air conditioners". *ORNL/TM-2015-536. Oak Ridge, TN: Oak Ridge National Laboratory. https://energy. gov/sites/prod/files/2015/10/f27/bto_pub59157_101515. pdf*.

AHRI, 2020. "AHRI Standard 540: Performance rating of positive displacement refrigerant compressors".

AIRAH, 2012. "Methods of calculating total equivalent warming impact(tewi) 2012".

ASHRAE, 1997. *ASHRAE Handbook - Fundamentals (SI Edition)*. merican Society of Heating, Refrigerating and Air-Conditioning Engineers, Inc, Atlanta.

Bell, I., 2012. "ACHP v1.4". URL `http://achp.sourceforge.net/index.html`.

Chen, W., 2008. "A comparative study on the performance and environmental characteristics of r410a and r22 residential air conditioners". *Applied thermal engineering*, Vol. 28, No. 1, pp. 1–7.

Churchill, S.W. and Bernstein, M., 1977. "A Correlating Equation for Forced Convection From Gases and Liquids to a Circular Cylinder in Crossflow". *Journal of Heat Transfer*, Vol. 99, No. 2, pp. 300–306.

Dabiri, A. and Rice, C., 1981. "A compressor simulation model with corrections for the level of suction gas superheat". *Ashrae Transactions*, Vol. 87, No. Part 2, pp. 771–782.

de Paula, C.H., Duarte, W.M., Rocha, T.T.M., de Oliveira, R.N. and Maia, A.A.T., 2020. "Optimal design and environmental, energy and exergy analysis of a vapor compression refrigeration system using R290, R1234yf, and R744 as alternatives to replace R134a". *International Journal of Refrigeration*, Vol. 113, pp. 10–20.

de Paula, C.H., Duarte, W.M., Rocha, T.T.M., de Oliveira, R.N. and Maia, A.A.T., 2021. "Energetic, exergetic, environmental, and economic assessment of a cascade refrigeration system operating with four different ecological refrigerant pairs". *International Journal of Air-Conditioning and Refrigeration*, Vol. 29, No. 03, p. 2150025.

Diniz, H.A., Paulino, T.F., Pabon, J.J., Maia, A.A. and Oliveira, R.N., 2021. "Dynamic model of a transcritical CO2 heat pump for residentialwater heating". *Sustainability (Switzerland)*, Vol. 13, p. 3464.

Duarte, W.M., 2018. *Numeric model of a direct expansion solar assisted heat pump water heater operating with low GWP refrigerants (R1234yf, R290, R600a and R744) for replacement of R134a*. Ph.D. thesis, UFMG.

Duarte, W.M., Paulino, T.F., Tavares, S.G., Cançado, K.N. and Machado, L., 2023. "Comparative study of geothermal and conventional air conditioner: A case of study for office applications". *Journal of Building Engineering*, Vol. 65, p. 105786.

Duarte, W.M., Pabon, J.J.G., Maia, A.A.T. and Machado, L., 2019. "Nonisentropic phenomenological model of a reciprocating compressor". *International Journal of Air-Conditioning and Refrigeration*, Vol. 27, No. 04, p. 1950039.

Encyclopaedia Britannica, 2022. "Montreal Protocol international treaty". URL `https://www.britannica.com/event/Montreal-Protocol`.

EPA, 2021. "International Treaties and Cooperation about the Protection of the Stratospheric Ozone Layer. ". U.S. Environmental Protection Agency, https://www.epa.gov/ozone-layer-protection/international-treaties-and-cooperation-about-protection-stratospheric-ozone, Accessed on 11 November 2022.

EPE, 2022. "National energy balance 2022, final report (in portuguese)". Empresa de Pesquisa Energética EPE, Rio de Janeiro, epe.gov.br/sites-pt/publicacoes-dados-abertos/publicacoes/PublicacoesArquivos/publicacao-675/topico-638/BEN2022.pdf. Accessed on 02 May 2023.

Fonseca, V.D., Duarte, W.M., de Oliveira, R.N., Machado, L. and Maia, A.A.T., 2022. "Mass flow prediction in a refrigeration machine using artificial neural networks". *Applied Thermal Engineering*, Vol. 214, p. 118893.

Garcia, J., Ali, T., Duarte, W.M., Khosravi, A. and Machado, L., 2018. "Comparison of transient response of an evaporator model for water refrigeration system working with R1234yf as a drop-in replacement for R134a". *International Journal of Refrigeration*, Vol. 91, pp. 211–222.

Gnielinski, V., 1976. "New equations for heat and mass transfer in turbulent pipe and channel flow". *Int. Chem. Eng.*, Vol. 16, No. 2, pp. 359–368.

Grimson, E.D., 1937. "Correlation and utilisation of new data on flow resistance and heat transfer for cross ow of gases over tube banks". *Trans. ASME*, Vol. 59, pp. 583–594.

Hughmark, G., 1965. "Holdup and heat transfer in horizontal slug gas-liquid ow". *Chemical Engineering Science*, Vol. 20, pp. 1007–1010.

Humia, G.M., Duarte, W.M., Pabon, J.J.G., de Freitas Paulino, T. and Machado, L., 2021. "Experimental study and simulation model of a direct expansion solar assisted heat pump to co2 for water heating: Inventory, coefficient of

performance and total equivalent warming impact". *Solar Energy*, Vol. 230, pp. 278–297.

Humia, G.M. *et al.*, 2022. *Estudo experimental e modelo de simulação do inventário de refrigerante em uma bomba de calor a CO2 dotada de evaporador solar*. Ph.D. thesis, Universidade Federal de Minas Gerais.

Incropera, F.P., DeWitt, D.P., Bergman, T.L. and Lavine, A.S., 2007. *Fundamentals of Heat and Mass Transfer*. LTC, 6th edition.

Kim, C.H. and Kim, N.H., 2021. "Evaporation heat transfer and pressure drop of the interim (r-448a, r-449a) and long term (r-455a, r-454c) low gwp r-404a alternative refrigerants in a smooth tube". *International Journal of Heat and Mass Transfer*, Vol. 181, p. 121903.

Lemmon, E.W., Bell, I.H., Huber, M. and McLinden, M., 2018. "Nist standard reference database 23: reference fluid thermodynamic and transport properties-refprop, version 10.0, national institute of standards and technology". *Standard Reference Data Program, Gaithersburg*.

Li, W., Chu, Y., Xu, P., Yang, Z., Ji, Y., Ni, L., Bao, Y. and Wang, K., 2017. "A transient model for the thermal inertia of chilled-water systems during demand response". *Energy and Buildings*, Vol. 150, pp. 383–395.

Makhnatch, P. and Khodabandeh, R., 2014. "Selection of low GWP refrigerant for heat pumps by assessing the life cycle climate performance (LCCP)". In *11th International Energy Agency Heat Pump Conference Montreal, May 12-16, 2014*.

Minetto, S., 2011. "Theoretical and experimental analysis of a CO_2 heat pump for domestic hot water". *International journal of refrigeration*, Vol. 34, No. 3, pp. 742–751.

Neils, G. and Klein, S., 2009. *Heat Transfer*. Cambridge university press.

Nunes, T.K., Vargas, J.V., Ordonez, J.C., Shah, D. and Martinho, L.C., 2015. "Modeling, simulation and optimization of a vapor compression refrigeration system dynamic and steady state response". *Applied Energy*, Vol. 158, pp. 540–555.

Otaki, T., 1971. "Holding refrigerant in refrigeration unit". In *Progress in Refrigeration Science and Technology. Proceedings of the XZZZ International Congress of Refrigeration, Washington, DC*. Vol. 2, pp. 535–544.

Paulino, T.F., Oliveira, R.N., Maia, A.A.T., Palm, B. and Machado, L., 2019. "Modeling and experimental analysis of the solar radiation in a CO_2 direct-expansion solar-assisted heat pump". *Applied Thermal Engineering*, Vol. 148, pp. 160 – 172.

Rabelo, S.N., Paulino, T.F., Machado, L. and Duarte, W.M., 2019. "Economic analysis and design optimization of a direct expansion solar assisted heat pump". *Solar Energy*, Vol. 188, pp. 164 – 174.

Rees, S., 2016. "An introduction to ground-source heat pump technology". In S.J. Rees, ed., *Advances in Ground-Source Heat Pump Systems*, Woodhead Publishing, pp. 1–25.

Sethi, A., Vera Becerra, E., Yana Motta, S.F. and Spatz, M.W., 2015. "Low GWP R22 replacement for air conditioning in high ambient conditions". *International Journal of Refrigeration*, Vol. 57, pp. 26–34. ISSN 01407007.

Shah, M.M., 2022a. "Improved correlation for heat transfer during condensation in mini and macro channels". *International Journal of Heat and Mass Transfer*, Vol. 194, p. 123069. ISSN 0017-9310.

Shah, M.M., 2022b. "New general correlation for heat transfer during saturated boiling in mini and macro channels". *International Journal of Refrigeration*, Vol. 137, pp. 103–116.

Tecumseh , 2023. "TSelect". URL `https://tselect.tecumseh.com/`.

UNEP, 2018. "2018 Report of the Refrigeration, Air Conditioning and Heat Pumps Technical Options Committee". URL `https://www.unep.org/ozonaction/who-we-are/about-montreal-protocol`.

Yang, B., Bradshaw, C.R. and Groll, E.A., 2013. "Modeling of a semi-hermetic CO2 reciprocating compressor including lubrication submodels for piston rings and bearings". *International Journal of Refrigeration*, Vol. 36, No. 7, pp. 1925–1937. ISSN 01407007.

Zhang, D., Wu, Q., Li, J. and Kong, X., 2014. "Effects of refrigerant charge and structural parameters on the performance of a direct-expansion solar-assisted heat pump system". *Applied Thermal Engineering*, Vol. 73, No. 1, pp. 522 – 528.

Zigrang, D. and Sylverster, N., 1982. "Explicit approximations to the solution of colebrook's friction factor equation". *AIChE Journal*, , No. 28, pp. 514–515.

7. RESPONSIBILITY NOTICE

The authors are solely responsible for the printed material included in this paper.